Novel pyrimidine-2,4-diamine derivative suppresses the cell viability and spindle assembly checkpoint activity by targeting Aurora kinases

Anna-Leena Salmela[1,2], Jeroen Pouwels[1], Jenni Mäki-Jouppila[1,3,4], Pekka Kohonen[1], Pauliina Toivonen[1], Lila Kallio[1] and Marko Kallio[1,3,5,*]

[1]VTT Technical Research Centre of Finland, Biotechnology for Health and Wellbeing, Turku, Finland, [2]Turku Graduate School of Biomedical Sciences, Finland, [3]Turku Centre for Biotechnology, University of Turku, Finland, [4]FinPharma Doctoral Program, Drug Discovery and Toxicology Section, Finland and [5]Centre of Excellence for Translational Genome-Scale Biology, Academy of Finland, Finland

*To whom correspondence should be addressed. Tel: +358-2-4788614; Fax: +358-20-722 2840;
Email: marko.kallio@vtt.fi

Mitosis represents a clinically important determination point in the life cycle of proliferating cells. One potential drug target within the mitotic machinery is the spindle assembly checkpoint (SAC), an evolutionarily conserved signaling pathway that monitors the connections between microtubules (MTs) and chromosomes. Mistakes in SAC signaling may lead to cell division errors that can trigger elimination of cancer cells at M phase or soon after exit from mitosis. In this study, we describe the cellular effects of a novel pyrimidine-2,4-diamine derivative that we discovered to inhibit the activity of SAC. The compound caused rapid escape from the mitotic arrest induced by lack of interkinetochore tension but not by lack of MT-kinetochore attachments. In cycling cells, the compound disrupted the architecture of mitotic spindle that triggered a transient M-phase arrest that was rapidly followed by a forced mitotic exit. The premature termination of M phase was found to be a consequence of precocious inactivation of SAC caused by a direct inhibitory effect of the compound on Aurora B kinase *in vitro* and in cells. The compound also targets Aurora A kinase and tubulin *in vitro* and in cells, which can explain the observed spindle anomalies. The reduced activity of Aurora B kinase resulted in polyploidy and suppression of cancer cell viability. Our data suggest that this new pharmacophore possesses interesting anticancer properties that could be exploited in development of mitosis-targeting therapies.

Introduction

The spindle assembly checkpoint (SAC) is a conserved mitotic signaling pathway that ensures equal segregation of chromosomes between the two daughter cells. SAC monitors microtubule (MT)-kinetochore interactions in early mitosis and prevents metaphase–anaphase transition until all chromosomes have proper attachments with the spindle MTs and their sister kinetochores are under tension (1,2). Partial inactivation of SAC leads to low levels of aneuploidy that has been associated with cancer initiation and progression, whereas complete inactivation of SAC results in massive genomic imbalance leading to elevated cancer cell death (3,4). These characteristics indicate that inhibitors of the SAC may have therapeutic potential. The current antimitotic cancer drugs are MT-targeting vinca alkaloids, taxanes and epothilones. Although these drugs have been very successful in clinics, their effects are not restricted to proliferating cells. Instead, they perturb MT-mediated processes also in resting and differentiated cells throughout the human body, which can cause adverse effects such as bone marrow suppression and neurotoxicity. Moreover, an increasing number of patients with MT-drug refractory tumors has

been encountered in the cancer clinics (5,6). These reasons among others have fueled the search for new anticancer drugs that would possess better cancer cell selectivity and fewer side effects.

Several key regulators of mitosis are overexpressed in human tumors. Whether this reflects the increased proliferation rate of tumor cells or true excess of particular mitotic protein in the cells is not fully explored. Nevertheless, mitotic proteins, especially those that contribute to SAC signaling, are potential drug targets as the survival of tumor cells may critically depend on their function or increased expression levels that the tumor cells have become addicted to. These options can provide a foundation for the design of drugs with enhanced cancer cell selectivity. In this study, we describe the characteristics and cellular targets of a compound 5-fluoro-2-*N*,4-*N*-diphenylpyrimidine-2,4-diamine, which we hereon call the spindle assembly checkpoint inhibitor 2 (SACi2) due to its capacity to overcome chemically activated SAC and induce cancer cell killing as a consequence of premature exit from mitosis.

Materials and methods

Cell culture

HeLa, A549, DU145, PC3 and MCF-10A cell lines growth mediums and culture conditions were described previously (7).

Chemicals and cell-based compound HTS

SACi2 (5-fluoro-2-*N*,4-*N*-diphenylpyrimidine-2,4-diamine, M_w = 280.3, Figure 1A) was obtained from ChemDiv (Chemdiv, San Diego, CA). All other chemicals were from Sigma (St Louis, MO) unless otherwise stated. SACi2 was prepared as a 25 mM stock solution in dimethyl sulfoxide (DMSO) and stored at –20°C. SACi2 was used in cell-based assays at 25 µM, MG132 at 20 µM, Ro31-8220 (Bisindolylmaleimide IX, LC Laboratories, Woburn, MA) at 5 µM, nocodazole at 70 nM, 350 nM and 3 µM, taxol (Molecular Probes, Sunnyvale, CA) at 600 nM, monastrol at 100 µM, vinblastine at 1 µM, MLN8054 at 0.5 µM (Selleck Chemicals, Houston), ZM447439 (Tocris Bioscience, Bristol, UK) and Z-VAD-FMK (Calbiochem, Billerica, MA) at 20 µM concentrations. The screen for small molecules that cause override from nocodazole induced mitotic block in HeLa cells was performed as described previously (8). The compound library screened contained 25 000 structurally diverse small molecules (ChemDiv). In short, 10 mM stock library plates were further diluted using Hamilton Microlab Star liquid handling robotics (Hamilton, Reno, NV) to 25, 5, 0.5 and 0.05 µM in growth medium. Cells were accumulated to M phase during overnight nocodazole incubation (350 nM). Mitotic cells were harvested by shake-off and replated on 384-well compound plates in culture medium containing nocodazole (final concentration 70 nM). Culture medium with 5 µM Ro 31-8220 (Bisindolylmaleimide IX, LC laboratories, Woburn, MA) and 70 nM nocodazole were used as a positive and negative control, respectively. After 4 h incubation, the wells were washed with a Tecan PW384 plate washer (Tecan, Groedig, Austria) to remove loosely attached mitotic cells. The remaining cells were fixed with 2 % paraformaldehyde in PHEM (60 mM PIPES, 25 mM N-2-hydroxyethylpiperazine-N'-2-ethanesulfonic acid, 10 mM ethylene-glycol-bis(aminoethylether)-tetraacetic acid, 4 mM MgSO4) containing 0.5 % Triton-100 and SYBR Gold nucleic acid stain (1:15 000, Molecular Probes). Fluorescence intensity of DNA was measured with Acumen Cell Cytometer using Acumen Explorer software (TTP LabTech Ltd, Melbourn, UK).

Live cell microscopy

HeLa H2B-GFP and HeLa cells growing on 35 mm live cell chambers (MatTek Corp., Ashland, MA) or multiwell plates were imaged using Zeiss Axiovert 200M microscopes equipped with 63× (NA 1.4) and 40× objectives, Orca-ER II (Hamamatsu Photonics, Hamamatsu city, Japan) and MetaMorph imaging software (Molecular Devices, Sunnyvale, CA) or AxioVision software. Images were captured at 5–10 min intervals with transmitted and/or fluorescence light.

Immunofluorescence, image acquisition and analysis

Immunofluorescence was performed as described earlier (9). We used primary antibodies against Aurora B/AIM1 (1:1000; Abcam, Cambridge, UK and 1:1000; BD Biosciences), Bub1 (1:200; Millipore, Billerica, MA), BubR1 (1:400; Abcam), CREST autoimmune serum (1:200; Antibodies, Davies, CA), Hec1 (1:200; Abcam), INCENP (1:500; Abcam), NuMA (1:8; gift from
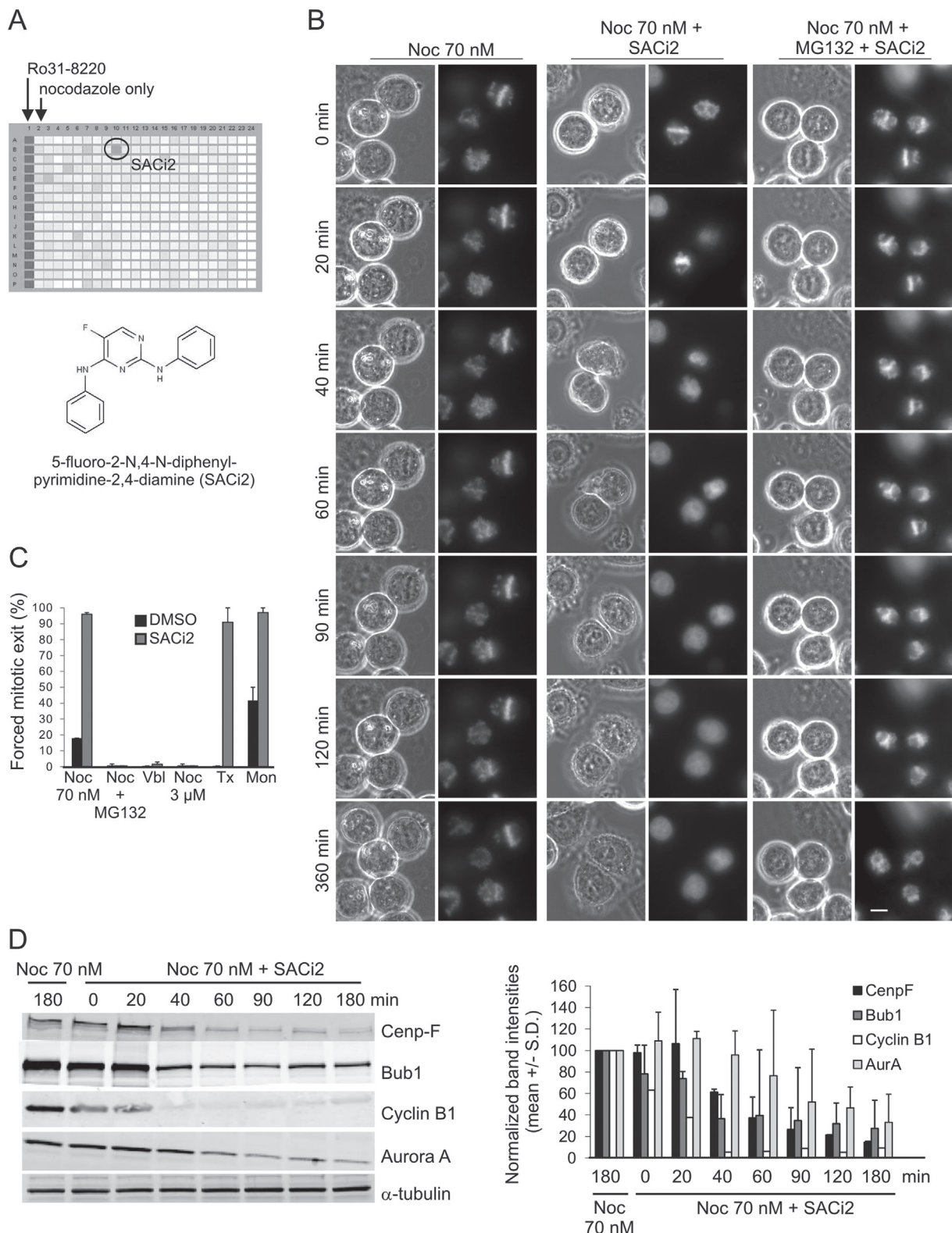
Fig. 1. SACi2 overcomes chemically induced mitotic block in a MT attachment and proteasome-dependent manner. (**A**) Position of SACi2 on the screen plate (circle) and the chemical structure of the compound. Ro31-8220 and nocodazole served as positive and negative control drugs, respectively, in the HTS. (**B**) Images from time-lapse films of HeLa-H2B-GFP cell populations treated with different chemicals. Left column: 70 nM nocodazole causes mitotic arrest persisting for several hours. Middle column: SACi2 rapidly forces nocodazole-arrested cells out of M phase. Right column: proteasome inhibitor MG132 prevents the SACi2-induced M-phase escape from nocodazole block. Scale bar = 10 μm. (**C**) SACi2 effects are dependent on MT-kinetochore attachments. The graph shows percentage of cells undergoing forced mitotic exit by SACi2 or DMSO in various pretreatment conditions (mean ± SEM, three independent assays). Nocodazole (Noc) was used at 70 nM and 3 μM, vinblastine (Vbl) at 1 μM, taxol (Tx) at 600 nM and monastrol (Mon) at 100 μM concentrations and were added 8 h before addition of DMSO or SACi2. MG132 (20 μM) was added 1 h before nocodazole. (**D**) The levels of Cenp-F, Bub1, Cyclin B1 and Aurora A decrease rapidly upon SACi2 induced forced mitotic exit (mean ± SEM, three independent assays). The data were normalized against the values from cell populations cultured in the presence of 70 nM nocodazole for 180 min.

M. Kallajoki), Aurora A pT288 (1:200; Cell Signaling), Aurora B pT232 (1:1000; Rockland), CenpA pSer7 (pCenpA, 1:500; Millipore), Histone H3 pSer10 (pHistH3, 1:3000; Upstate), Pericentrin (1:2000; Abcam), Survivin (1:300; Abcam), α-tubulin (1:2000; Abcam) and γ-tubulin (1:200; Abcam). Secondary fluorescein isothiocyanate, Cy3- or Cy5-conjugated antibodies were used at 1:600–1:800 (Jackson ImmunoResearch, West Grove, PA). Images of the fixed cells were acquired using Zeiss Axiovert 200M platform and MetaMorph software as Z-stacks with 0.3 μm step sizes. Quantification of kinetochore protein signals was done as described elsewhere (9). For each experiment, a minimum of 50 kinetochores was analyzed in at least five cells per condition. Signal intensities of Aurora B pT232 and Histone H3 pSer10 were quantified at whole cell level and normalized against CREST signal intensities in 10 cells per each of the two independent experiments. Aurora A pT288 signal intensities at spindle poles were quantified and normalized against γ-tubulin signal intensities in a minimum of 10 cells per each of the two independent experiments. The quantification of MT filaments in the cells after exposure to cold buffer in the presence of SACi2, DMSO or taxol followed by α-tubulin immunofluorescence was performed using the Metamorph as follows. The background of maximum projections made of image stacks representing through cell focus series was flatten and a threshold including only the microtubule filaments (α-tubulin staining) was set. The integrated intensity of the filaments was measured and compared between the treatment groups.

In vitro kinase assay

The *in vitro* kinase assays to determine if SACI2 inhibits Aurora B, Aurora A and Cdk1/Cyclin B were performed as described previously (8).

Western blotting

Preparation of cell extracts, sodium dodecyl sulfate–polyacrylamide gel electrophoresis and immunoblotting were done as described elsewhere (9). We used antibodies against Aurora A (1:1000; Abcam), Aurora B (1:1000; Abcam), Bub1 (1:2000; Abcam), CenpF (1:1000; BD Biosciences), cleaved poly (ADP ribose) polymerase (PARP) (1:1000; Cell Signaling), Cyclin B1 (1:500; BD Biosciences), p-Histone H3 S10 (1:3000; Upstate), INCENP (1:1000; a gift from E. Nigg), p-Aurora A T288 (1:1000; Cell Signaling), Survivin (1:400; Abcam), glyceraldehyde 3-phosphate dehydrogenase (1:30 000; Advanced ImmunoChemicals) and α-tubulin (1:1000; Abcam). IR Dye® Conjugated secondary antibodies (Rockland Immunochemicals, Gilbertsville, PA) were used at 1:5000. Signals were detected using Odyssey Infrared Imaging System (LI-COR Biotechnology, Lincoln, NE).

Fluorescence-activated cell sorting

Harvesting of cells and fluorescence-activated cell sorting (FACS) analysis were performed as described previously (7). The data were collected with the BD FacsArray™ (BD Biosciences) and analyzed using FCS Express 3 (De Novo Software, Los Angeles, CA).

In vitro tubulin polymerization assay

Fluorescence-based *in vitro* tubulin polymerization assay (BK011, Cytoskeleton) was performed as described previously (7). SACi2 was used at 0.5, 5, 15 and 25 μM concentrations. Taxol (3 μM), vinblastine (3 μM) and DMSO were used as controls. Tubulin polymerization was recorded at 1 min intervals for 60 min at 37°C with excitation at 355 nm and emission at 460 nm by Victor 1420 Multilabel HTS Counter (PerkinElmer).

Colony formation assay

MCF-10A cells were cultured on 24 well plates, 120 cells per well. Next day, medium was replaced with fresh medium supplemented with DMSO or SACi2 (25 μM). After 3 days, fresh medium including DMSO or SACi2 was changed and incubation was continued for 3 more days before release into control medium for the last 3 days. The cells in the wells were fixed at two time points (days 3 and 9) with methanol for 15 min on ice, washed with phosphate-buffered saline (PBS) and stained with 0.05% crystal violet for 30 min followed by two washes with PBS and water.

Monastrol treatments, spindle architecture assays and drug washouts

Cells growing on coverslips were treated with monastrol for 4h and fixed with 2% paraformaldehyde containing 0.5% Triton-X 100 and 0.2% glutaraldehyde. Parallel samples incubated with monastrol were first treated with MG132 for 1h before addition of DMSO or SACi2 for 2h in the continued presence of monastrol and MG132. For monastrol washout experiment, the cells were fixed directly from monastrol block or subjected to a washout (3×10min washes in presence of MG132) and released into MG132-containing medium supplemented with DMSO or SACi2. After 1h incubation also, these cells were fixed and immunostained with antibodies against NuMA and Pericentrin (spindle poles and centrosomes were analyzed in 50 cells per each individual treatment). For spindle analysis, cells were treated with MG132 for 1h followed by addition of DMSO or SACi2 for 2h or vice versa. Cells were fixed as described above and immunostained with antibodies against NuMa and Pericentrin. About 50 cells in each of

two independent experiments were analyzed. In SACi2 washout experiment, cells treated with MG132 and SACi2 were washed 4×5min in presence of MG132. The cells were fixed after 2h recovery and stained with anti-α-tubulin antibodies.

Statistical testing

Analyses were performed with Student's *t*-test and *P* values <0.050 were considered significant.

Results

SACi2 overrides chemically induced mitotic arrest in a proteasome-dependent manner

Identification of small compounds overriding a chemically induced mitotic arrest was based on a previously designed methodology (8,10). The HTS of a library containing 25 000 structurally diverse low molecular weight molecules led to the identification of SACi2 (Figure 1A) that was further characterized using various cell-based and *in vitro* assays. HeLa H2B-GFP cells were cultured 8 h in a medium containing 70 nM nocodazole and immediately after the addition of SACi2 or vehicle (DMSO) were subjected to time-lapse microscopy. The majority (82%, *n* = 95 out of 116) of nocodazole arrested and DMSO-treated cells remained in mitosis for at least 6 h (Figure 1B and C, Supplementary Video 1, available at *Carcinogenesis* Online). In sharp contrast, the majority (97%, *n* = 151 out of 155) of nocodazole blocked and SACi2-treated cells underwent a rapid escape from M phase (Figure 1B and 1C, Supplementary Video 2, available at *Carcinogenesis* Online). The mitotic cells decondensed their chromosomes and changed their morphology from round into adhered within 2 h after SACi2 addition. The induction of mitotic escape by SACi2 was not a cell line-specific phenotype as it was also observed in prostate cancer PC3 (74% exit rate) and DU145 (66% exit rate) cells and in non-malignant MCF-10A breast epithelial cells (73% exit rate).

To exclude the possibility that the SACi2-treated cells exhibited a premature chromosome decondensation rather than a premature M-phase exit, we analyzed the expression levels of Aurora A, Bub1, Cyclin B1 and Cenp-F in nocodazole-arrested cells exposed to SACi2 (Figure 1D). The levels of these proteins are normally notably decreased upon exit from mitosis. Analysis of nocodazole blocked and SACi2 cotreated cell populations showed that cyclin B1 levels dropped dramatically by 40 min after SACi2 addition. The levels of Aurora A, Bub1 and Cenp-F declined rapidly about 1 h after addition of SACi2 in comparison with nocodazole-arrested cells. The decline in the mitotic markers coincided with the SACi2-induced chromosome decondensation and morphological conversion of cells indicating forced exit from M phase.

The molecular target of SAC is the activity of a mitotic ubiquitin ligase termed the anaphase-promoting complex/cyclosome (APC/C) (11) that directs anaphase inhibitors such as securin and cyclin B1 for a proteasome-mediated degradation soon after SAC inactivation. The proteasome activity is hence downstream of the APC/C but required for the mitotic exit (12,13). To investigate whether SACi2 suppresses SAC signaling or acts downstream of the APC/C, we treated nocodazole-arrested HeLa H2B-GFP cells with a proteasome inhibitor MG132 for 1 h before addition of SACi2 or DMSO and subsequent time-lapse imaging (Figure 1B, Supplementary Video 3, available at *Carcinogenesis* Online). All nocodazole-MG132-DMSO- (*n* = 135) and all nocodazole-MG132-SACi2-treated cells (*n* = 156) remained at M phase for at least 6 h indicating that SACi2 induced forced mitotic exit depends on proteasome activity. Supporting the notion, proteasome inhibition prevented the degradation of mitotic markers in the SACi2-treated cells (Supplementary Figure S1, available at *Carcinogenesis* Online). This suggests that SACi2 is not causing a general shut down of mitosis, but rather targets processes upstream of the proteasome activity.

SACi2 causes escape from mitotic arrest induced by lack of tension but not lack of MT-kinetochore attachments

In the presence of 3 μM nocodazole, which causes complete depolymerization of MTs, none of the SACi2-treated mitotic

cells escaped mitosis (n = 76) indicating that SACi2 can overcome the checkpoint only when MTs are attached to kinetochores (Figure 1C). In line with this, SACi2 caused escape from mitosis in the majority of cells arrested at M phase with MT-stabilizing drug taxol (82%, n = 133 out of 162) or Eg5-inhibitor monastrol (14) (99%, n = 87 out of 88) but not in cell populations treated with 1 µM vinblastine (3%, n = 2 out of 66), a MT-destabilizing drug that completely disrupts MTs at this concentration (Figure 1C). Together, these observations suggest that SACi2 can override the SAC induced by lack of interkinetochore tension but is not able to impair the arrest induced by lack of MT-kinetochore attachments.

SACi2 interferes with kinetochore accumulation of key SAC regulators and inhibits Aurora kinases activity in vitro and in cells

The cellular phenotype induced by SACi2 raised the questions whether the compound interferes with kinetochore targeting of key SAC proteins. We analyzed two mitotic kinases, Bub1 and BubR1, that are central components of the SAC (15). HeLa cells arrested in mitosis with 70 nM nocodazole were treated for 1 h with MG132 prior to 3 h incubation with SACi2 in the continued presence of nocodazole. Control cells blocked at mitosis with nocodazole were incubated for 4 h with MG132. The cells were subsequently fixed and immunostained for Bub1, BubR1 and Hec1 followed by quantification of the levels of these proteins at the kinetochores (Figure 2A and 2B). The analysis showed that the kinetochore accumulation of Bub1 and BubR1 were significantly reduced in the SACi2-treated cells (both proteins were down by 86%, ***P < 0.001), potentially explaining the impairment of the SAC in these cells. Importantly, SACi2 did not change the amount of Hec1 at the kinetochores (Figure 2A and 2B, reduced by 2%), indicating that the general architecture of the kinetochore was not affected.

The activity of Aurora B kinase is required for the correction of improper MT-kinetochore interactions and the maintenance of SAC signaling when sister kinetochores are attached to MTs but are not under tension (16–18). Next, using the same assay conditions described above we investigated the effects of SACi2 on the cellular localization of Aurora B. Opposed to the control cells where Aurora B localized at the inner centromeres, mitotic cells treated with SACi2 showed Aurora B staining along the chromosome arms (Figure 2C). To clarify whether the other subunits in the Aurora B complex [the chromosomal passenger complex (CPC)] were also mislocalized, we immunostained the SACi2-treated cells with anti-INCENP and anti-survivin antibodies. Both INCENP and survivin signals were spread along the chromosome arms suggesting that the whole CPC was mislocalized by SACi2. We quantified and compared the SACi2-induced CPC mislocalization to the effects of ZM447439, a well-characterized Aurora inhibitor (16,19), and noticed a similar erroneous localization of the CPC (Figure 2C). Finally, we determined the protein levels of the three CPC subunits in nocodazole and MG132-pretreated cells exposed to SACi2 or ZM447439. We observed only minor variations in the protein levels of Aurora B, INCENP and survivin between the different treatments proposing that neither SACi2 nor ZM447439 change the protein amount of the CPC subunits (Figure 2D).

To determine if SACi2 directly inhibits the activities of Aurora kinases, we performed an *in vitro* kinase assay in which γ-32P incorporation into myelin basic protein (MBP) by recombinant Aurora kinases A and B was analyzed in the presence of different SACi2 concentrations (Figure 3A). The autoradiograph showed that SACi2 inhibited both Aurora kinases at concentrations that cause escape from mitosis. From the results, we have estimated that the IC_{50} for Aurora A and Aurora B inhibition by SACi2 is about 15 µM. Importantly, the activity of Cdk1 was not inhibited at any concentration of SACi2 used in this experiment (Figure 3A). Together, these data suggest that SACi2 interferes with SAC signaling through direct inhibition of Aurora kinases A and B.

To investigate if SACi2 treatment interferes with cellular functions of Aurora kinases, we stained the compound-treated cells with antibodies recognizing Aurora B phoshorylated at T232 (pAurB, an

autophosphorylated marker epitope for kinase activity) (20), Histone H3 phosphorylated at S10 (pHistH3, an epitope phosphorylated by Aurora B) (17), CenpA phosphorylated at S7 (pCenpA, an epitope phosphorylated by Aurora B) (21) and Aurora A phosphorylated on T288 (pAurA, an autophosphorylated epitope marking kinase activity) (22). Quantification of the phospho-antibody signal intensities (Figure 3B) showed that SACi2 highly significantly reduced the centromere located pAurB (down by 32%, ***P < 0.001), centromere located pHistH3 (down by 72%, ***P < 0.001), centromere located pCenpA (down by 97%, ***P < 0.001) and spindle pole located pAurA (down by 96%, ***P < 0.001) in comparison with the controls. The decrease in phospho-antibody signal intensities were comparable with the reduction induced by ZM447439 and Aurora A inhibitor MLN8054 (Figure 3B). We confirmed the SACi2 induced loss of phospho-antibody signal intensities using western blotting. Both the pHistH3 and pAurA were significantly reduced in the SACi2-treated cell populations (Figure 3C). Also the positive control drugs ZM447439 and MLN8054 reduced pHistH3 and pAurA levels, respectively, which was comparable with the SACi2 effect (Figure 3C). Importantly, SACi2, ZM447439 or MLN8054 did not notably change the total amount of Aurora kinases when compared with the DMSO controls (Figure 2D and 3C). We conclude that SACi2 severely compromises the function of Aurora kinases in cells and *in vitro*.

Cycling cells at M phase exhibit premature mitotic exit and cytokinesis defects when treated with SACi2

To test if SACi2 induces premature mitotic exit in unperturbed cycling cells, DMSO or SACi2 was added to HeLa H2B-GFP cells after which they were imaged using time-lapse microscopy (Figure 4). The control mitotic cells (n = 30) underwent a normal chromosome segregation and cytokinesis (Figure 4, upper row). In sharp contrast, cells exposed to SACi2 at early mitosis (prophase and prometaphase, n = 25) were instantly forced out of M phase without any attempt to execute chromosome segregation or cytokinesis (Figure 4, middle row, Supplementary Video 4, available at *Carcinogenesis* Online). Similarly, the cells exposed to SACi2 in metaphase exited mitosis without chromosome segregation and failed in cytokinesis (n = 25, Figure 4, bottom row, Supplementary Video 5, available at *Carcinogenesis* Online). Interestingly, the cells that were at the borderline of entering anaphase or in early anaphase at the time of SACi2 administration (n = 10) segregated the sister chromatids but with mistakes (anaphase chromosome bridges) and aborted cytokinesis that led to the formation of binucleate progeny cells (Figure 4, bottom row). This data are in concordance with the reported consequences of Aurora B inhibition: cells rapidly and prematurely exit mitosis with impaired cytokinesis (16,17).

Pre-mitotic cells treated with SACi2 show impaired mitotic progression and perturbation of chromosome movements and spindle architecture after entry into M phase

HeLa cells were treated with SACi2 or DMSO and the cells entering M phase were monitored using time-lapse microscopy. These cells exposed to SACi2 at G_2 phase failed in chromosome alignment and exhibited a transient M-phase delay followed by a forced mitotic exit without cytokinesis (Figure 5A). The average length of mitosis (nuclear envelope breakdown-to-late telophase) in these cells was 190.0 ± 11.6 min (n = 50) in comparison with 64.3 ± 3.4 min (n = 52) of the controls (Figure 5C). Analysis of the HeLa H2B-GFP cells exposed to SACi2 at G_2 phase confirmed the transient M-phase delay and forced mitotic exit without cytokinesis (Figure 5B). Also evident were the limited chromosome movements in the cells entering mitosis in the presence of SACi2: the chromosomes rapidly pooled together into a tight mass of chromatin that eventually decondensed upon the premature exit from mitosis (Figure 5B).

To get insights into the reasons for the transient mitotic delay, we pretreated HeLa cells with MG132 for 1 h and added SACi2 or DMSO to the culture medium for additional 2 h. The cells were then fixed and stained with an anti-α-tubulin antibody. Analysis of the spindle

architecture showed that the SACi2-treated cells rarely formed bipolar spindles (13%, $n = 38$). Instead, the cells were mainly multipolar with three or more MT-organizing centers (87%, $n = 254$ out of 292 cells, Figure 5D). Besides the several main spindle poles, the SACi2-treated cells often had small satellite MT foci in the cytosol (Figure 5D). In the vehicle-treated control population only 7% of the cells exhibited multiple poles (Figure 5D). In a second set of assays, we washed out SACi2 from the cells and cultured them in the presence of MG132 for
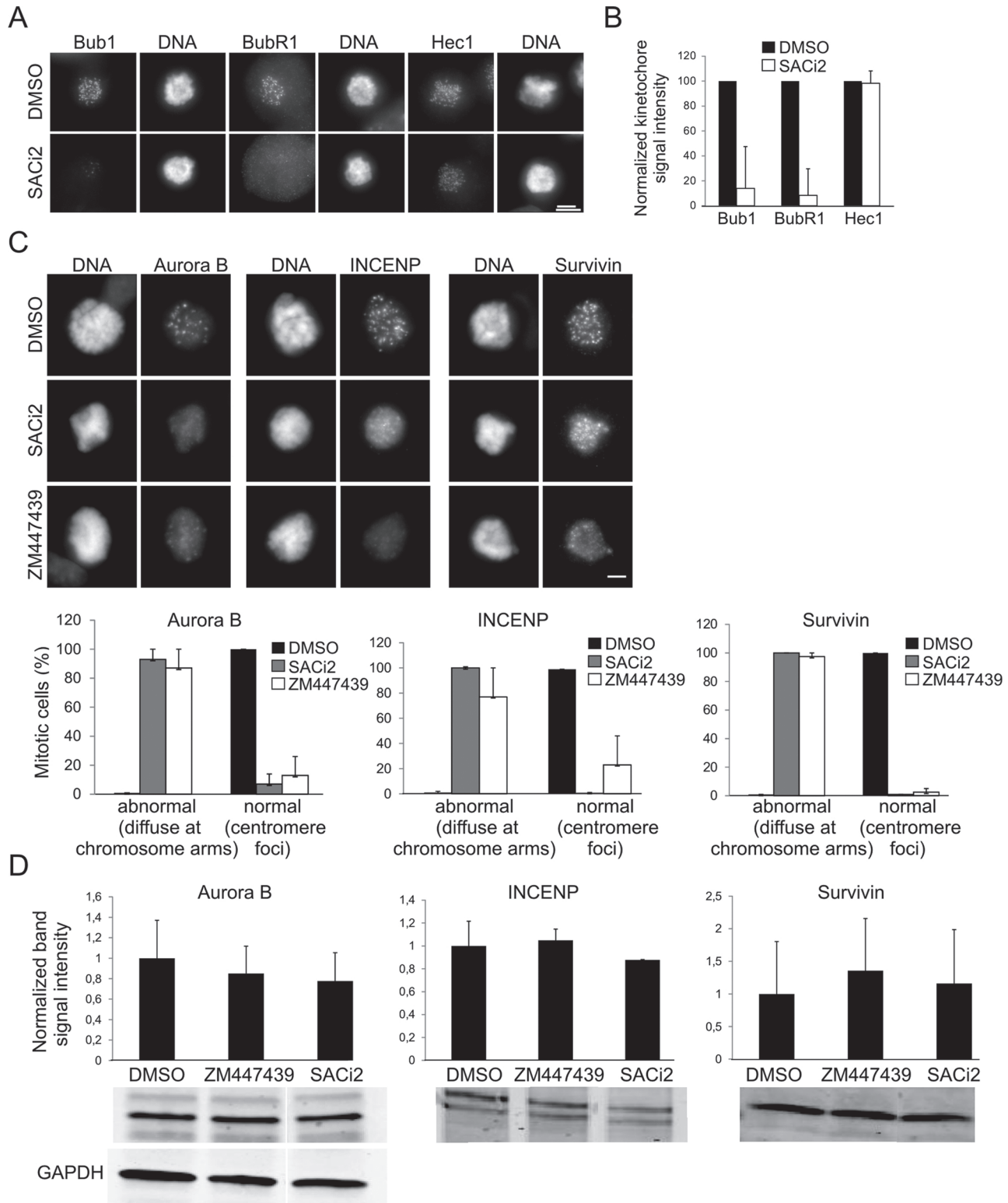

Fig. 2. SACi2 perturbs kinetochore localization of Bub1 and BubR1 and mislocalizes CPC from the centromeres. (**A**) Micrographs showing immunolocalization of Bub1, BubR1 and Hec1 in nocodazole-arrested mitotic cells cotreated with DMSO or SACi2 for 3 h. (**B**) Normalized kinetochore fluorescence intensities of the proteins (mean ± SEM, two independent assays). (**C**) Subcellular localization of CPC subunits after various drug treatments for 3 h (mean ± SEM, two independent assays). (**D**) Quantification of CPC subunit levels in nocodazole-arrested and DMSO, SACi2 or ZM447439 cotreated cells (mean ± SEM, two independent assays). MG132 was added in all experiments 1 h before the other drugs to prevent mitotic exit.
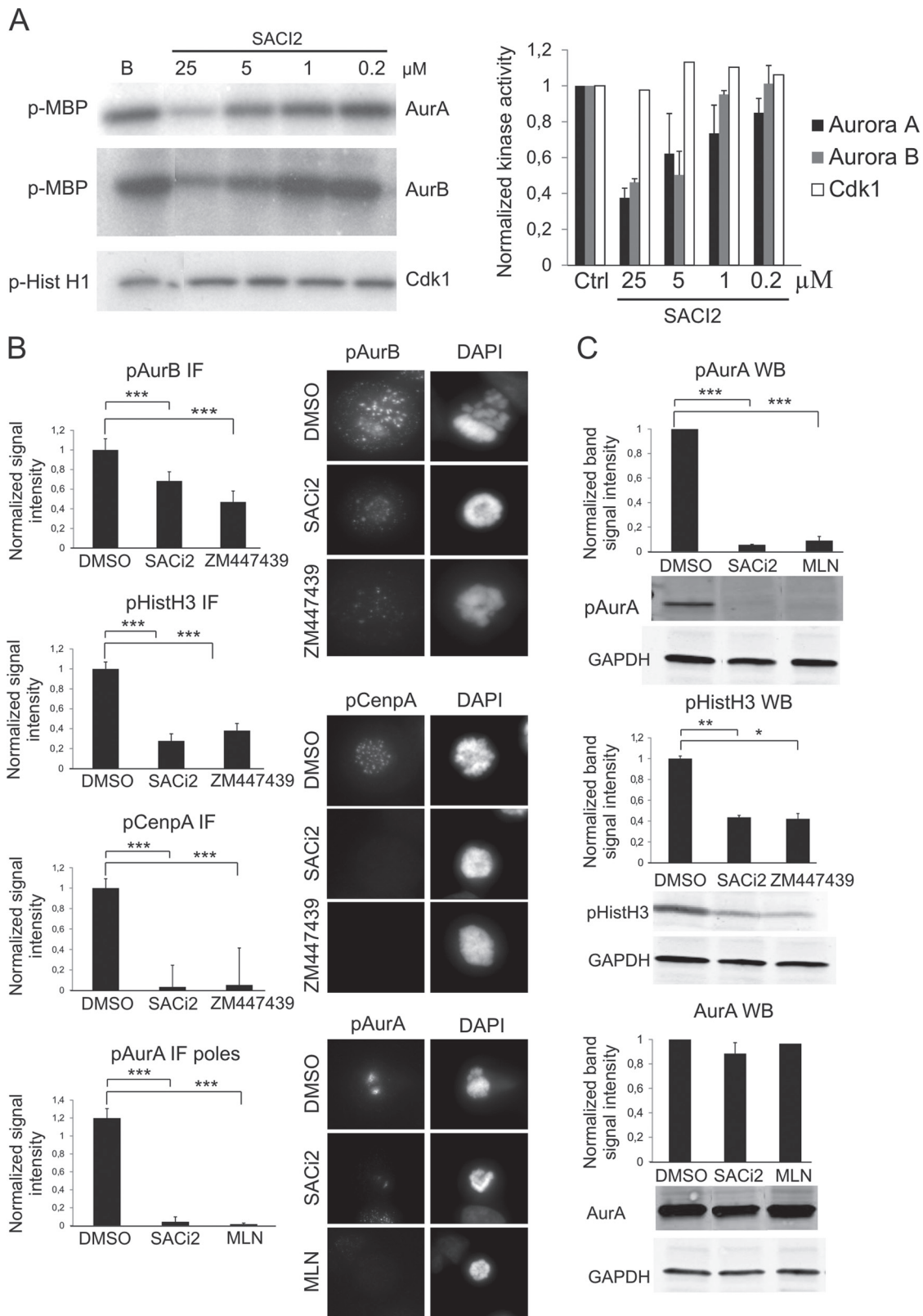
Fig. 3. SACi2 inhibits Aurora A and B kinases *in vitro* and in cells. **(A)** Autoradiograph of *in vitro* kinase assay (mean ± SEM, two independent assays). The remaining kinase activity is shown relative to control reaction without SACi2. The graph shows the band signal intensities after background subtraction. The estimated IC_{50} for Aurora A and Aurora B inhibition by SACi2 is about 15 μM. **(B)** Normalized fluorescence signal intensities of pAurB, pHistH3 and pCenpA at centromeres (all normalized against CREST signal intensity), and pAurA at spindle poles (normalized against γ-tubulin signal intensity) in cells treated with indicated drugs (mean ± SEM, two independent assays). The micrographs show representative cells stained with pAurB (upper panel), pCenpA (middle panel) and pAurA (lower panel) antibodies after various drug treatments. **(C)** Quantification of pAurA, pHistH3 and AurA protein levels in nocodazole-arrested cell populations cotreated with DMSO, SACi2, ZM447439 or MLN8054 (mean ± SEM, two independent assays). MG132 was used to prevent mitotic exit. Glyceraldehyde 3-phosphate dehydrogenase served as a loading control. SACi2 was used at 25 μM concentration (B and C).
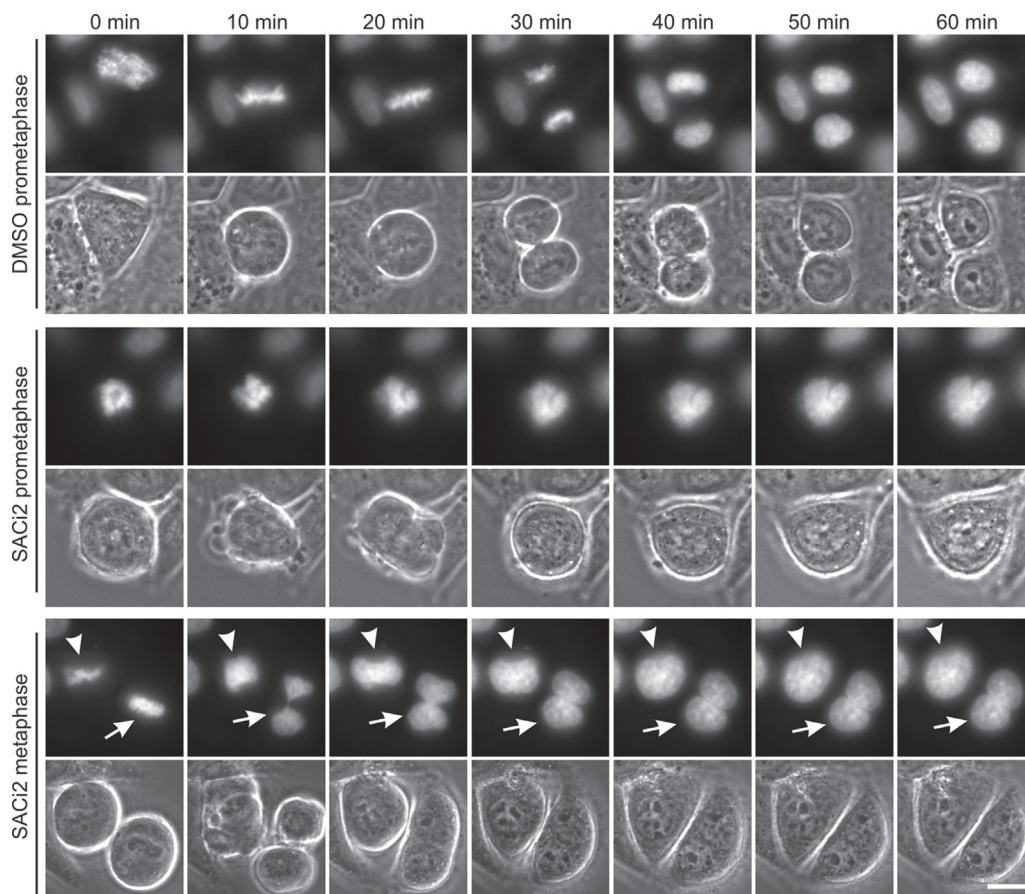
Fig. 4. Mitotic cells exposed to SACi2 rapidly exit M phase without cytokinesis. Control cells (DMSO, upper panel) undergo normal chromosome segregation and cytokinesis within 1 h. Cells exposed to SACi2 at prometaphase (middle panel) or metaphase (bottom panel, white arrowhead) rapidly decondense the chromosomes and exit M phase without execution of chromosome segregation and cytokinesis. A cell exposed to SACi2 at the metaphase–anaphase transition (bottom panel, white arrow) separates the sister chromatids with mistakes (anaphase bridge) and initiates cytokinesis that is aborted leading to formation of a binucleate progeny cell. Scale bar = 10 µm.

2 h before fixation and examination of the spindle architecture. These cells were able to fully recover from the SACi2 treatment and form bipolar spindles with normal chromosome alignment indicating that the compound effects are reversible (Figure 5D).

To further characterize the SACi2-induced spindle anomalies we compared the compound effects to those of ZM447439. Analysis of the NuMA and pericentrin signals indicated that both SACi2 and ZM447439 caused multipolarity (Supplementary Figure S2A–C, available at *Carcinogenesis* Online). Moreover, SACi2 induced a notable increase in the number of small NuMA-positive but pericentrin-negative acentrosomal foci (Supplementary Figure S2A–C, available at *Carcinogenesis* Online). Finally, a spindle reassembly experiment indicated that the majority of the cells recovering from monastrol treatment in the presence of SACi2 formed two pericentrin-positive spindle poles (74%, $n = 37$ out of 50 cells) but also exhibited many NuMa-positive and pericentrin-negative small satellite MT foci (72%, $n = 36$ out of 50 cells; Supplementary Figure S2D, available at *Carcinogenesis* Online), whereas in the control cells, 42 out of 50 cells (84%) had two pericentrin positive poles and none had small satellite foci. Importantly, 2 h incubation of monastrol pretreated mitotic cells with a cocktail of SACi2 and MG132, in the continued presence of monastrol, did not notably change the spindle architecture: the majority of these cells remained monopolar (data not shown).

SACi2 influences tubulin polymerization in vitro and MT stability in cells

The observed defects in chromosome behavior and spindle architecture prompted us to investigate whether SACi2 directly influences the

MTs. To this end, we tested the compound effects on tubulin polymerization *in vitro*. The results demonstrate that SACi2 perturbed the tubulin incorporation by stabilizing the process (Supplementary Figure S3, available at *Carcinogenesis* Online). To investigate whether SACi2 has an impact on MT stability in cells, we measured compound's potency to rescue MTs from cold buffer-induced depolymerization. Cells exposed to cold culture buffer for 15, 30 and 45 min in the presence of SACi2 preserve more MT filaments compared with the DMSO controls (Supplementary Figure S4, available at *Carcinogenesis* Online). Although the MT-stabilizing effect of SACi2 in cells was statistically significant at 45 min time point in comparison with controls (*$P < 0.05$), it was only moderate in comparison with taxol. These results suggest that parts of the cellular phenotype induced by the compound can be due to the effects on MT dynamics.

SACi2 induces polyploidy and apoptosis

To determine if SACi2 influences the ploidy and cell viability, we cultured five cell lines in the presence of DMSO or SACi2 for 1, 3 or 5 days before cell harvest and analysis of their morphology and DNA profiles. At day 1, SACi2 induced an increase in G_2/M population in all cell lines. This is in line with the observed transient mitotic delay and forced mitotic exit without cytokinesis, which caused formation of polyploid G_1 cells (Figure 6A). At days 3 and 5, some of the cells were highly polyploid (8N-16N) indicating that the polyploidy further increased during time (Figure 6A and 6B). Furthermore, SACi2 increased the number of cells with fragmented nuclei (sub-G_1 population) and decreased the total number of cells indicating that the drug caused cell death in all five cell lines examined (Figure 6A).
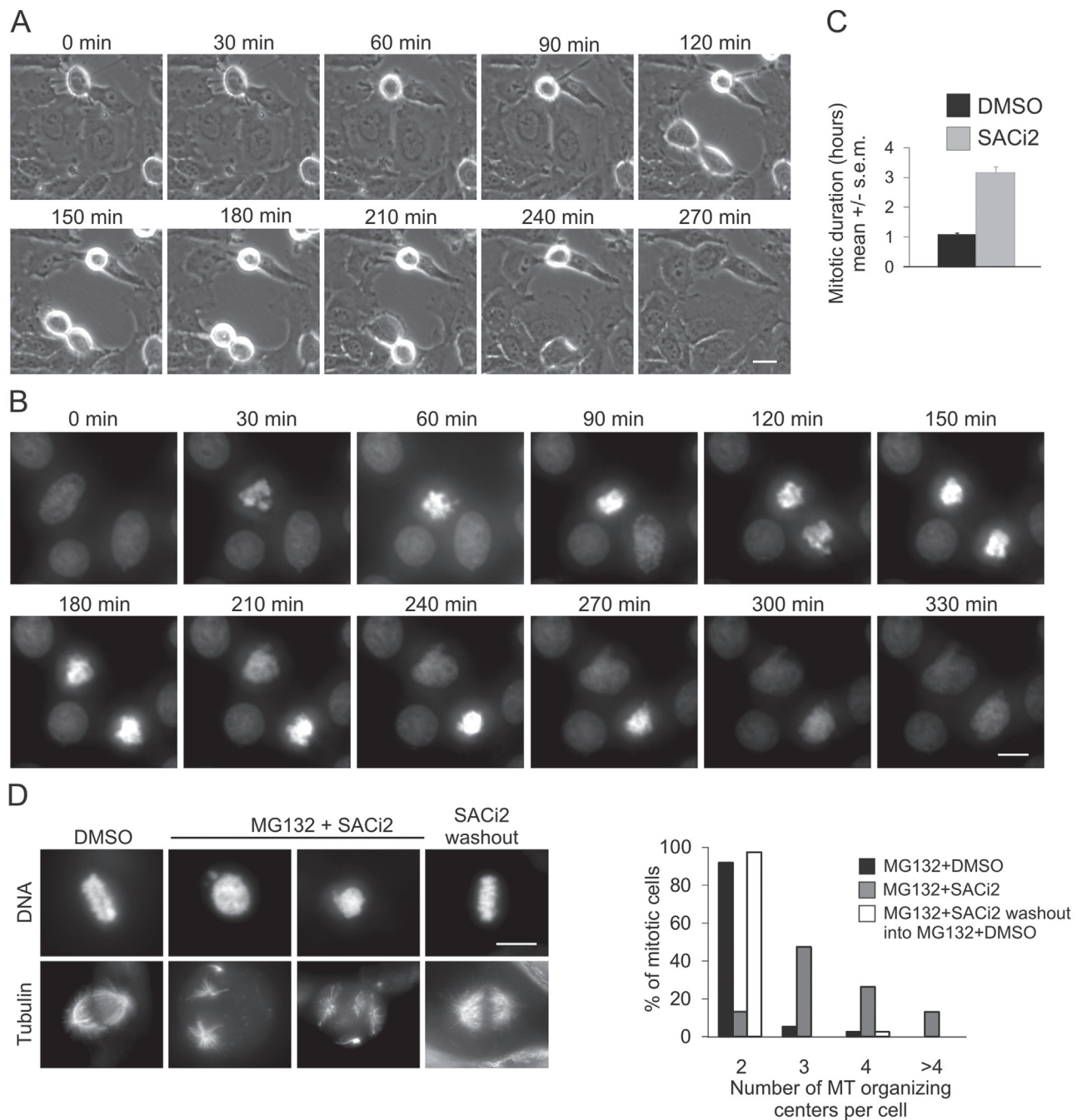
442

Fig. 5. Hela (**A**) and HeLa H2B-GFP (**B**) cells exposed to SACi2 at G$_2$ phase exhibit a transient M-phase delay with massive chromosome misalignment followed by forced mitotic exit without cytokinesis. (**C**) Average duration of HeLa cell mitosis after exposure to SACi2 or DMSO at G$_2$ phase (mean ± SEM, two independent assays). (**D**) Metaphase cells exposed to SACi2 become multipolar but can reorganize a bipolar spindle upon washout of the compound. MG132 was used to prevent premature mitotic exit. The graph shows number of MT organizing foci in cells after drug treatments. Scale bars = 10 µm.

Interestingly, the mode of cell death was different in tumorigenic HeLa and non-tumorigenic MCF-10A cells: in HeLa cells PARP was cleaved indicative of caspase-mediated apoptosis, whereas in MCF-10A cells PARP was intact (Figure 6C). Inhibition of caspases with Z-VAD-FMK prevented SACi2-mediated cell death in HeLa cells (Figure 6D). These observations prompted us to investigate the fate of MCF-10A cells using a colony formation assay. At day 3 after addition of SACi2, the surviving MCF-10A cells had become multinucleated and polyploid, and were incapable of forming colonies. Importantly, the ploidy of these cells was limited to 4N-8N (Figure 6A, Supplementary Figure S5, available at *Carcinogenesis* Online). Washout of SACi2 at day 6 did not trigger population regrowth during

the next 3 days, which suggests that MCF-10A cells may have entered cellular senescence after the first erroneous mitoses (Supplementary Figure S5, available at *Carcinogenesis* Online). Altogether, our data indicate that SACi2 induces polyploidy and cell death in all cell lines examined and may drive senescence in a cell type-dependent manner.

Discussion

The clinical success of current antimitotic cancer drugs such as taxanes is based on their capacity to perturb MT-dependent processes and trigger cell death upon induction of cell cycle anomalies. This phenomenon involves the SAC that is responsible for the M-phase delay
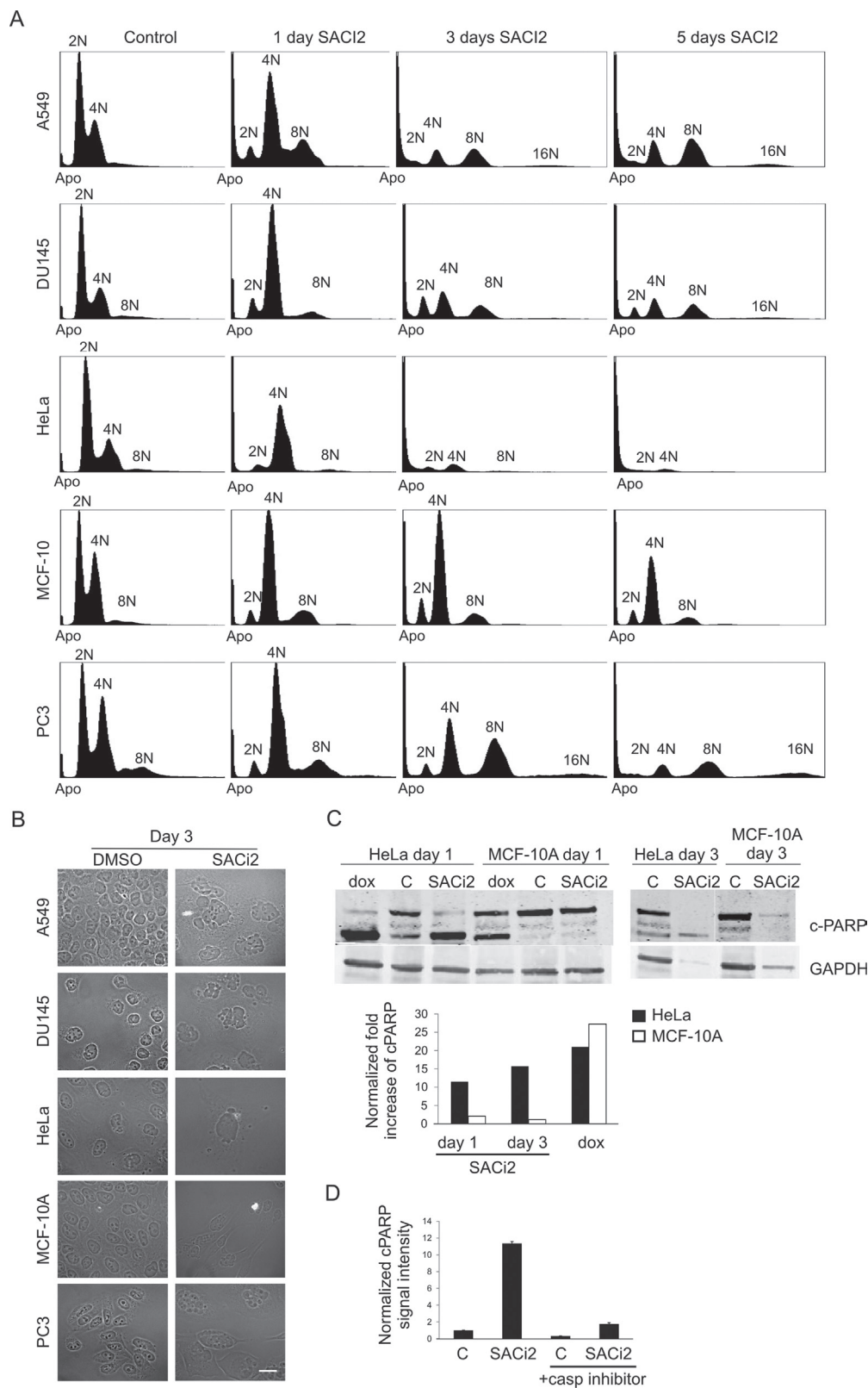
443

Fig. 6. SACi2 induces polyploidy and cell death in cells. (**A**) FACS analysis of five cell lines treated with DMSO or SACi2 for 1, 3 or 5 days. (**B**) Phase contrast images of DMSO- and SACi2-treated cells at day 3. Scale bar = 20 µm. (**C**) Mode of cell death by SACi2 is different between HeLa and MCF-10A cells. Western blots of PARP cleavage (c-PARP) and glyceraldehyde 3-phosphate dehydrogenase (loading control) at days 1 and 3 in both cell lines after indicated drug treatments. The graph shows normalized fold increase of c-PARP. Doxorubicin (dox) was used as a positive control for induction of apoptosis. (**D**) HeLa cells were treated with caspase inhibitor Z-VAD-FMK for 1h followed by DMSO or SACi2. The graph shows normalized c-PARP signal intensities at day 1.

induced in response to defects in the mitotic spindle function (11). Recent studies have clarified a dual role of SAC in tumorigenesis: low levels of chromosome instability caused by SAC mistakes can provide growth advantage for the tumor cells, whereas massive aneuploidy

raised as a result of full inactivation of the SAC kills most cancer cell types (3,4). The latter phenomenon creates an intriguing option for drug discovery within the mitotic machinery. Future pharmacophores targeting the SAC proteins may allow the development of cancer cell-specific therapies and means to suppress the growth of taxane refractory tumors.

Aurora B kinase is absolutely required for normal SAC signaling and ordered chromosome segregation (23). Also Aurora A kinase has essential tasks in dividing cells (23), although the outcome of its functional perturbation is typically masked by the more dominant phenotype of Aurora B inhibition. Aurora kinases are frequently found overexpressed in many human tumors (24,25) that may point to the clinical vulnerability of tumors cells and provide relevant strategies for their inhibition. To date, a plethora of Aurora inhibitors have been discovered, some of which have advanced to clinical trials (26,27). Our data demonstrate that the main consequence of SACi2 is a rapid and precocious exit from M phase without cytokinesis, which results in polyploidy and induction of cell death that is the major cause for suppression of cell growth. The phenotype mimics the classical outcome of Aurora B kinase inhibition suggesting that this kinase is the primary target of the compound.

Our original cell-based screen was designed to identify compounds that target proteins controlling the activity of the SAC. Earlier, we have reported the discovery of two screen hit compounds of plant origin, fisetin and eupatorin, both of which inhibited Aurora B (7,8). In light of our previous data and this study, our HTS platform appears to be especially well suited for the identification of Aurora inhibitors. Aurora inhibitors, fisetin and eupatorin, are structurally very similar, whereas the structure of SACi2 is completely different. Therefore, we speculate that the ATP-pocket of Aurora kinases is accessible for structurally diverse compounds. Alternatively, eupatorin and fisetin may bind to sites distinct from SACi2. The discovery that SACi2 also influences tubulin polymerization *in vitro* is in line with the observed multipolarity and extra satellite MT foci in cells, which is a typical outcome of MT-stabilizing drugs (28). Pyrimidine derivatives have been reported to target Aurora kinases (29,30), but the impact of these compounds on tubulin is unknown.

In summary, we have discovered a novel pharmacophore that interestingly targets both MTs and critical SAC proteins, the Aurora kinases, *in vitro* and in cells. The multiple cellular targets of SACi2 and its structural differences in comparison with other Aurora inhibitors encourage for the chemical optimization of SACi2 as well as warrant the examination of its effects in more complex models such as taxane-resistant cell lines.

Supplementary material

Supplementary Figures 1–5 and Supplementary Videos 1–5 can be found at http://carcin.oxfordjournals.org/.

Funding

Acknowledgements

References

1. Maresca,T.J. *et al.* (2010) Welcome to a new kind of tension: translating kinetochore mechanics into a wait-anaphase signal. *J. Cell. Sci.*, **123**(Pt 6), 825–835.

2. Musacchio,A. (2011) Spindle assembly checkpoint: the third decade. *Philos. Trans. R. Soc. Lond., B, Biol. Sci.*, **366**, 3595–3604.

3. Kops,G.J. *et al.* (2004) Lethality to human cancer cells through massive chromosome loss by inhibition of the mitotic checkpoint. *Proc. Natl. Acad. Sci. U.S.A.*, **101**, 8699–8704.

4. Weaver,B.A. *et al.* (2008) Low rates of aneuploidy promote tumorigenesis while high rates of aneuploidy cause cell death and tumor suppression. *Cell. Oncol.*, **30**, 453.

5. Schmidt,M. *et al.* (2007) Mitotic drug targets and the development of novel anti-mitotic anticancer drugs. *Drug Resist. Updat.*, **10**, 162–181.

6. Zhou,J. *et al.* (2005) Targeting microtubules for cancer chemotherapy. *Curr. Med. Chem. Anticancer. Agents*, **5**, 65–71.

7. Salmela,A.L. *et al.* (2012) The flavonoid eupatorin inactivates the mitotic checkpoint leading to polyploidy and apoptosis. *Exp. Cell Res.*, **318**, 578–592.

8. Salmela,A.L. *et al.* (2009) Dietary flavonoid fisetin induces a forced exit from mitosis by targeting the mitotic spindle checkpoint. *Carcinogenesis*, **30**, 1032–1040.

9. Pouwels,J. *et al.* (2007) Shugoshin 1 plays a central role in kinetochore assembly and is required for kinetochore targeting of Plk1. *Cell Cycle*, **6**, 1579–1585.

10. DeMoe,J.H. *et al.* (2009) A high throughput, whole cell screen for small molecule inhibitors of the mitotic spindle checkpoint identifies OM137, a novel Aurora kinase inhibitor. *Cancer Res.*, **69**, 1509–1516.

11. Musacchio,A. *et al.* (2007) The spindle-assembly checkpoint in space and time. *Nat. Rev. Mol. Cell Biol.*, **8**, 379–393.

12. Potapova,T.A. *et al.* (2009) Fine tuning the cell cycle: activation of the Cdk1 inhibitory phosphorylation pathway during mitotic exit. *Mol. Biol. Cell*, **20**, 1737–1748.

13. Skoufias,D.A. *et al.* (2007) Mitosis persists in the absence of Cdk1 activity when proteolysis or protein phosphatase activity is suppressed. *J. Cell Biol.*, **179**, 671–685.

14. Mayer,T.U. *et al.* (1999) Small molecule inhibitor of mitotic spindle bipolarity identified in a phenotype-based screen. *Science*, **286**, 971–974.

15. Elowe,S. (2011) Bub1 and BubR1: at the interface between chromosome attachment and the spindle checkpoint. *Mol. Cell. Biol.*, **31**, 3085–3093.

16. Ditchfield,C. *et al.* (2003) Aurora B couples chromosome alignment with anaphase by targeting BubR1, Mad2, and Cenp-E to kinetochores. *J. Cell Biol.*, **161**, 267–280.

17. Hauf,S. *et al.* (2003) The small molecule Hesperadin reveals a role for Aurora B in correcting kinetochore-microtubule attachment and in maintaining the spindle assembly checkpoint. *J. Cell Biol.*, **161**, 281–294.

18. Lens,S.M. *et al.* (2003) The survivin/Aurora B complex: its role in coordinating tension and attachment. *Cell Cycle*, **2**, 507–510.

19. Girdler,F. *et al.* (2008) Molecular basis of drug resistance in aurora kinases. *Chem. Biol.*, **15**, 552–562.

20. Walter,A.O. *et al.* (2000) The mitotic serine/threonine kinase Aurora2/AIK is regulated by phosphorylation and degradation. *Oncogene*, **19**, 4906–4916.

21. Zeitlin,S.G. *et al.* (2001) CENP-A is phosphorylated by Aurora B kinase and plays an unexpected role in completion of cytokinesis. *J. Cell Biol.*, **155**, 1147–1157.

22. Yasui,Y. *et al.* (2004) Autophosphorylation of a newly identified site of Aurora-B is indispensable for cytokinesis. *J. Biol. Chem.*, **279**, 12997–13003.

23. Vader,G. *et al.* (2008) The Aurora kinase family in cell division and cancer. *Biochim. Biophys. Acta*, **1786**, 60–72.

24. Kollareddy,M. *et al.* (2008) Aurora kinases: structure, functions and their association with cancer. *Biomed. Pap. Med. Fac. Univ. Palacky. Olomouc. Czech. Repub.*, **152**, 27–33.

25. Mountzios,G. *et al.* (2008) Aurora kinases as targets for cancer therapy. *Cancer Treat. Rev.*, **34**, 175–182.

26. Cheung,C.H. *et al.* (2009) Aurora kinase inhibitors in preclinical and clinical testing. *Expert Opin. Investig. Drugs*, **18**, 379–398.

27. Lens,S.M. *et al.* (2010) Shared and separate functions of polo-like kinases and aurora kinases in cancer. *Nat. Rev. Cancer*, **10**, 825–841.

28. Hornick,J.E. *et al.* (2008) Live-cell analysis of mitotic spindle formation in taxol-treated cells. *Cell Motil. Cytoskeleton*, **65**, 595–613.

29. Aliagas-Martin,I. *et al.* (2009) A class of 2,4-bisanilinopyrimidine Aurora A inhibitors with unusually high selectivity against Aurora B. *J. Med. Chem.*, **52**, 3300–3307.

30. Wang,S. *et al.* (2010) Discovery of N-phenyl-4-(thiazol-5-yl)pyrimidin-2-amine aurora kinase inhibitors. *J. Med. Chem.*, **53**, 4367–4378.